POLITECNICO DI TORINO
Repository ISTITUZIONALE

Strengthening RC Slabs with CFRP Bars Using the Plastic Limit Method to Control Plastic Deformation

Original
Strengthening RC Slabs with CFRP Bars Using the Plastic Limit Method to Control Plastic Deformation / Sharhan, Z.S., Cucuzza, R., Domaneschi, M., Movahedi Rad, M.. - 59:(2024), pp. 96-104. (7th International Conference on Material Strength and Applied Mechanics, MSAM 2024 Gyor (Hun) 29 July 2024 through 1 August 2024) [10.3233/ATDE240532].

Availability:
This version is available at: 11583/2996517 since: 2025-01-10T20:45:24Z

Publisher:
IOS Press

Published
DOI:10.3233/ATDE240532

Terms of use:

This article is made available under terms and conditions as specified in the corresponding bibliographic description in the repository

Publisher copyright

(Article begins on next page)

25 June 2026

Material Strength and Applied Mechanics
A. Khotsianovsky and Y. Chen (Eds.)
© 2024 The Authors.
This article is published online with Open Access by IOS Press and distributed under the terms of the Creative Commons Attribution Non-Commercial License 4.0 (CC BY-NC 4.0).
doi:10.3233/ATDE240532

Strengthening RC Slabs with CFRP Bars Using the Plastic Limit Method to Control Plastic Deformation

Zahraa Saleem SHARHAN [a], Raffaele CUCUZZA [b], Marco DOMANESCHI [b], and Majid MOVAHEDI RAD [a,1]

[a] *Department of Structural and Geotechnical Engineering, Széchenyi István University, H-9026 Győr, Hungary*
[b] *Department of Structural, Building and Geotechnical Engineering, Politecnico Di Torino, Corso Duca degli Abruzzi, 24 - 10129 Torino, Italy*

Abstract. The objective of this work is to improve the punching strength and control the plastic deformation of two-way reinforced concrete (RC) slabs using carbon fiber reinforced polymer (CFRP) bars. The efficacy of this reinforcement technique was evaluated by constructing four reinforced concrete flat slabs. One specimen was utilized as a reference slab, while the other three specimens were reinforced using the Near Surface Mounted (NSM) CFRP bars approach. The slabs, which had identical dimensions and steel reinforcement, were exposed to patch load, and tested until they reached the point of failure. For evaluating the strength of two-way reinforced concrete (RC) slabs, the Concrete Plastic Damage (CDP) constitutive model was developed and implemented. CFRP bars are inserted into the slab at a depth from the tension face to enhance their strength. The investigation commences with the calibration of a numerical model utilizing data obtained from laboratory experiments. This will be achieved by establishing an advanced analytical method that incorporates the plasticity of concrete damage and the use of CFRP bars, along with a multiplier to determine the plastic limit load. Numerical simulations are employed to investigate shear dynamics by including diverse elements. The results showed that an increase in the ratio of strengthening had a significant effect on shear strength.

Keywords. CFRP bars, strengthening, two-way slab, plastic limit, CDP model.

1. Introduction

Historically, concrete constructions were believed to have near-permanent strength and endurance. Recently, there has been a significant rise in the degradation and destruction of these buildings, necessitating immediate repair and strengthening [1]. Throughout time, several methods to enhance strength have been created and utilized, gaining a level of approval. The utilization of FRP reinforcement is becoming important in repairing and enhancing RC structures. Akhundzada et al. [2], Abdel-Kareem [3], and Hasan Meisami et al. [4] explored the effect of using the CFRP bars in strengthening the concrete slabs, the results demonstrated that ultimate load capacity was increased using CFRP reinforcement. This reinforcement delayed the start of early concrete cracking, sustaining

[1] Corresponding Author: Majid MOVAHEDI RAD, E-mail: majidmr@sze.hu.

a linear relationship at greater loads between load displacement and deformation. Moreover, CFRP reinforcement enhanced the flexural stiffness and sustained strong adhesion with the concrete under loading conditions. Other relevant studies by Behzard et al. [5] and Foret [6] developed a nonlinear three-dimensional numerical model to forecast the flexural properties of the analyzed slabs which strengthened with CFRP bars, and it was observed that experimental data and numerical results exhibited a positive correlation.

The Concrete Damage Plasticity (CDP) model, a continuum derived from the plasticity damage model, has raised serious problems. Cement-based materials theories make extensive use of the CDP model because of its capacity to account for modulus degradation and predictive performance through irreversible plastic deformation [7]. Carol et al. [8] investigated various configurations of plasticity and damage in 2001. Rad et al. [9] also explored these configurations. Gatuingt et al. [10] conducted a study using isotropic degradation to examine different combinations of plasticity types. Similarly, Kratzig et al. [11] investigated the same topic in 2004.

The objective of this work is to control the plastic deformation of two-way RC slabs reinforced with CFRP bars by conducting an optimal elastoplastic analysis. The study focuses on the application of a plastic limit load multiplier and the control of damage plasticity in concrete using CFRP. It was essential to validate numerical models by comparing them to laboratory test results, particularly in ensuring the accuracy of the strengthening ratio. Subsequently, perform a set of simulations according to the given limitations. The CDP model was employed to calibrate the numerical model to simulate the concrete damage that ensued. Evaluating the impact of load multipliers on concrete damage by transitioning from elastic to plastic analysis. Each of these parameters was considered, and their impacts were analyzed.

2. Constitutive Model of Concrete

To estimate the concrete's inelastic behavior, the CDP model integrates isotropic damaged elasticity, compressive plasticity, and tensile plasticity. The total strain value ε is composed of two sections: the elastic component $\varepsilon^{el}$and the plastic section ε^{pl}, as explained below [12]:

$$\varepsilon = \varepsilon^{el}.\sigma = D^{el} \tag{1}$$

$$\sigma = D^{el} : (\varepsilon - \varepsilon^{pl}) \tag{2}$$

$$D^{el} = (1-d)D_0^{el} \tag{3}$$

$$\bar{\sigma} = D_0^{el} : (\varepsilon - \varepsilon^{pl}) \tag{4}$$

Eq. (2) can be reformulated as follows, considering the nominal stress and utilizing the decreased elastic tensor illustrated in Eq. (3):

$$\sigma = (1-d)D_0^{el} : (\varepsilon - \varepsilon^{pl}) \tag{5}$$

Following the stress–strain relationship, the CDP model of damage plasticity was developed:

$$\sigma = (1-d)\,.\,\overline{\sigma} \rightarrow \sigma = (1-d_t)\,.\,\bar{\sigma}_t + (1-d_c).\,\overline{\sigma}_c \tag{6}$$

The variables representing scalar damage, are denoted as $d_t$and d_c, vary between Zero (indicating no damage) and one (indicating complete damage). Tensile cracking and compressive compression were fundamentally incorporated into the damage model that was applied to concrete.

As demonstrated in Figure 1 [12], plasticity damage impacts uniaxial tension and compression responses. Under compression and tension load, the CDP model predicts the behavior of concrete in uniaxial tensile and compression situations as follows:

$$\sigma_t = (1 - d_t).E_0.(\varepsilon_t - \varepsilon_t^{pl,h}) \tag{7}$$

$$\sigma_c = (1 - d_c).E_0.(\varepsilon_c - \varepsilon_c^{pl,h}) \tag{8}$$

Therefore, to calculate the active tension and compression stresses, σ_t and σ_c, the subsequent formulas are applied:

$$\bar{\sigma_t} = \left(\frac{\sigma_t}{(1-d_t)}\right) = E_0.(\varepsilon_t - \varepsilon_t^{pl,h}) \tag{9}$$

$$\bar{\sigma_c} = \left(\frac{\sigma_C}{(1-d_c)}\right) = E_0.(\varepsilon_c - \varepsilon_c^{pl,h}) \tag{10}$$

In this context, the tensile strain ε_t is defined as $\varepsilon_t^{pl,h} + \varepsilon_t^{el}$, and the compressive strain ε_c is equal to $\varepsilon_c^{pl,h} + \varepsilon_c^{el}$.

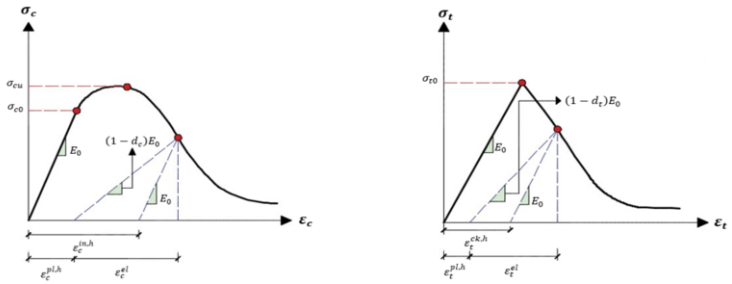

Figure 1. The response of concrete to uniaxial loading: (left) Under Compression, (Right) Under Tension[12].

3. Applying the plastic limit analysis static principles

Design models and plastic analysis that integrate residual stresses utilize this method, as numerous structure types have successfully incorporated complementary strain energy [13]. As a constraint on structural failure, it is utilized in this investigation. In situations where energy quantity constraints are required to control residual configurations, an appropriate computational approach was developed to integrate the strain energy of residual forces into a comprehensive assessment of plastic behavior. Residual forces consisting of the following generate the additional strain energy:

$$W_p = \frac{1}{2E} \sum_{i=1}^{n} \frac{l_i}{A_i} N_i^{R^2} \leq W_{p0} \tag{11}$$

where, W_{p0}represents the maximum amount of energy that can be extracted from the structure's elastic strain energy to derive W_p. The components of the bar material are represented as follows: E represents Young's modulus; N_i^R signifies the bar member's

residual force; A_i is the area of the cross-section of a bar element, where $(i = 1, 2, \ldots., n)$ and so on. Eq. (11) incorporates the concept of a limit value W_{p0} to account for deformations of plastic rebar. The residual forces N^{pl} observed in the structure after discharging are characterized by two additional forces, namely the elastic internal force N^{el}, and the interior plastic force N^{pl}, which arises when the load P_0 is applied.

4. Experimental work

To investigate the efficacy of utilizing CFRP rods to reinforce two-way RC slabs, an experimental program was initiated. For the investigation, four identical slabs were constructed. All the slabs had a focused load applied to it and supported at both ends. Each slab measured (1200 x 1200 x130) mm, as depicted in Figure 2. The slabs were designated as G1, G2 and G3, with G0 serving as the control. The parametric study was designed for near-surface mounted bars strengthening. G1 was strengthened with 3 CFRP bars, G2 with 5 CFRP bars, and G3 with 7 CFRP bars, all CFRP bars were 6 mm diameter at each direction, Table 1. detailed the mechanical characteristics of CFRP bars.

Laboratory experiments were conducted to evaluate concrete properties, with four samples analyzed for each test after a 28-day curing period. Concrete compressive strength was measured using three 150x300 mm cylinders and three 150 mm slabs. After 28 days of curing, these specimens were tested for tension and compression to get the average concrete values. Table 2 shows concrete cube and cylinder compressive strengths. The assessments encompassed the behavior in compression and tension, as shown in Figure 3. The primary tensile reinforcement in all specimens consisted of 15 steel bars with 10 mm diameter at a space of 61 mm between each other, while the compression reinforcement comprised 12 steel bars with 6 mm diameter at a space of 85 mm between each other. The specific attributes of the reinforcements are expounded upon in Table 3.

Table 1. Properties of CFRP Bars

Type of strengthening	**CFRP Bar**
Properties	
Elongation (mm)	1.7
Tensile strength (MPa)	2704
Modulus of Elasticity (GPa)	163
Diameter of the bar (mm)	6

Table 2. Concrete's compressive strength

Slab Specimens	**Average Compressive Strength (MPa) at (28 days)**	
	f c`	f_{cu}
G0	30	36
G1	31	37
G2	30	36.1
G3	29	36.27

Table 3. Characteristics of reinforcing bars

Properties	Ø 10 mm	Ø 6 mm
Yield Stress (MPa)	486	335
Modulus of Elasticity (MPa)	195	192
Ultimate Stress (MPa)	480	620

5. Test response of concrete slabs

Table 4 displays the values for ultimate load (Pu), cracking load (Pcr), width of crack (Wcr) at Pu, and deflections (Δv) at the Pu. Slab G0 was tested without using CFRP bars.

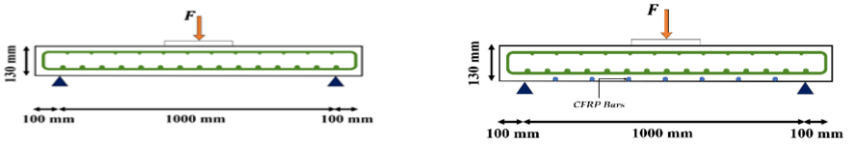

Figure 2. Typical slab specimen (Left) Control slab without strengthening, (Right) Strengthened Slabs with CFRP

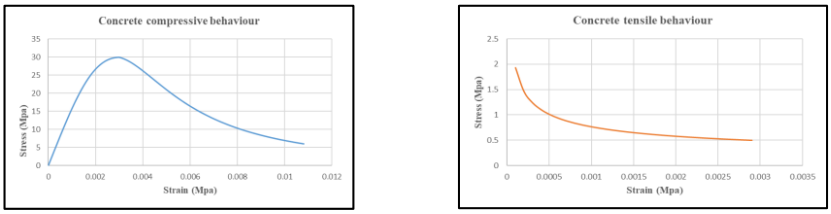

Figure 3. Experimental properties of concrete: (Left) in Compression, (Right) in Tension

During the experiment, the slab's reaction was carefully watched while the load was gradually raised. Until the initial cracking appeared, the slab the slab specimen demonstrated elastic behavior through the initial phase of testing.

When a 120 kN load was placed to the region of constant moment, the initial fractures appeared. Under constant load, the specimen had flexural cracks that originated in its interior and propagated toward the edges, rapidly increasing in width. Slab G0 experienced flexural collapse when subjected to a load of 241 kN, characterized by a quick and sustained rise in deflection despite the load being constant. The process of strengthening with CFRP bars involved the attachment of CFRP to the underside of the slabs using grooves that were 18 mm deep and 10 mm wide. Initial observation of cracking occurred in G1 at a load of 180 kN, followed by G2 at 199 kN, and G3 at 225 kN. The G1, G2, and G3 slabs failed due to punching mode at loads of 442 kN, 480 kN, and 541 kN, respectively. When comparing the control slab G0 to slabs G1, G2, and G3, there were noticeable rises in ultimate loads of 83.4%, 99%, and 124% correspondingly.

The correlation between the applied load and the severity of damage is apparent, as the escalation in load results in elevated early stresses in both the concrete and steel constituents. The importance of the corresponding strain energy in the process of plastic degradation is emphasized. Handling this component skillfully lowers plastic deterioration and failure. The data shows CFRP-reinforced slabs failed punching. The results show that CFRP may increase slab load-bearing capacity and reduce center deflection and fracture breadth under the same loads.

Table 4. The results obtained from the slabs' experimental testing

Slab Specimens	Pcr (kN)	Δv (mm)	Wcr (mm)	Pu (kN)	Pcr/ Pu	Pu/ Pu.Control	Pcr/ Pcr.Control
G0	120	11.2	1.4	241	0.49	1	1
G1	180	10	0.9	442	0.40	1.834	1.5
G2	199	9.5	0.8	480	0.414	1.99	1.65
G3	225	9	0.76	541	0.415	2.24	1.875

6. Numerical modelling

To characterize the nonlinear behavior of CFRP-bar-reinforced two-way RC slabs, finite element analysis was used. CDP was used in the study. Modeling used four Two-way RC slabs, one control slab without CFRP and three slabs reinforced with CFRP bars in different ratios were used to construct these slabs. The concrete slab was simulated using an 8-node solid element (C3D8R), while the reinforcing rods were represented using 2-node linear beam elements (T3D2). By utilizing an embedded region, the bond between concrete and reinforcements was simulated. In accordance with the ABAQUS manual, the bond between CFRP bars and concrete was also represented by embedded region in the model.

A pin support for rotation at one end and a roller support for rotation and horizontal movement at the other end were identified as boundary conditions. To mitigate local failure resulting from compression, steel bearing plates measuring (250 x 250 x 25) mm were systematically positioned, the modeling approach utilized the (C3D8R) 8-node solid element. Furthermore, to replicate the experimental conditions, A concentrated vertical load was applied in the middle of the slab directly on the steel plate. As well as achieving precision, a narrow lattice was implemented, which caused the slabs to contain an estimated total of 21600 elements. A 20-mesh size produced the best degree of accuracy when the effects of several mesh sizes on numerical precision and computing efficiency were examined.

The CDP dataset detects tensile cracking and compressive crushing as failure modes based on specimen mechanical property testing. These properties allow ABAQUS to generate CDP parameters, accurately representing concrete damage behavior. The data in Table 5 is used to calculate the CDP plasticity parameters after sensitivity studies. CDP settings must be constant during optimization. The numerical models calibrated using ABAQUS showed significant agreement with test results, proving the model's efficacy in predicting the performance of two-way RC slabs with CFRP rods. As shown in Figure 4, tension damage patterns are similar, with CFRP bars reducing red damaged regions in the flexural section (the green lines on the slabs indicate the location of CFRP bars that are embedded within the depth of the slab), proving the comparability of the experimental and numerical results. Figure 5 illustrates the load-deflection properties of the control slab G0 in comparison to the G1, G2, and G3 specimens, offering additional proof that the results acquired from experimental and numerical approaches are consistent, both in terms of experimentation and simulation.

The highest load and lowest crack width are in Slab G3. CFRP-reinforced slabs punched, while slab G1 deboned. These data demonstrate that CFRP increases slab load-bearing capacity and reduces crack center and width deflection under similar loads.

Table 5. Concrete CDP data

Angle of Dilation	Fb0 / fc0	Eccentricity	k	k
31	1.16	0.2	0	0.001

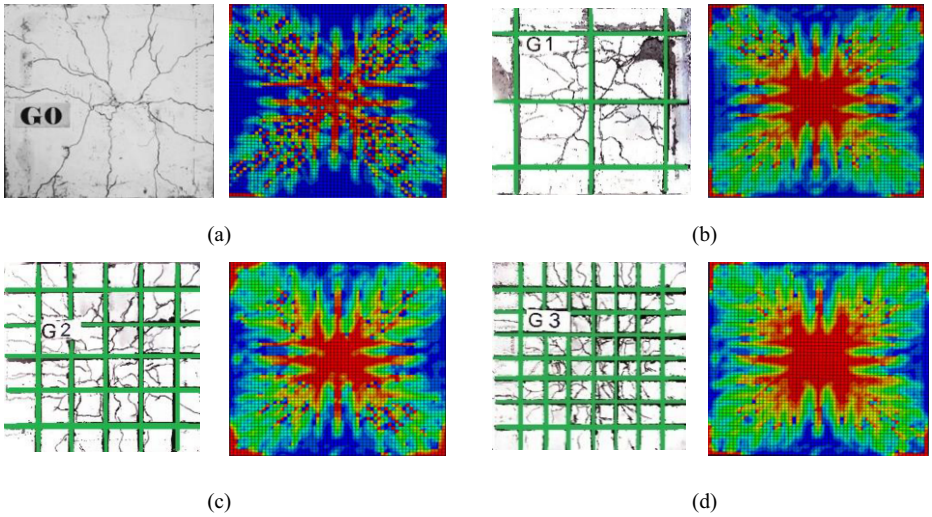

Figure 4. Numerical and Experimental Damage Patterns Comparison, (a) Control slab without CFRP, (b) Slab G1, (c) Slab G2, (d) Slab G3

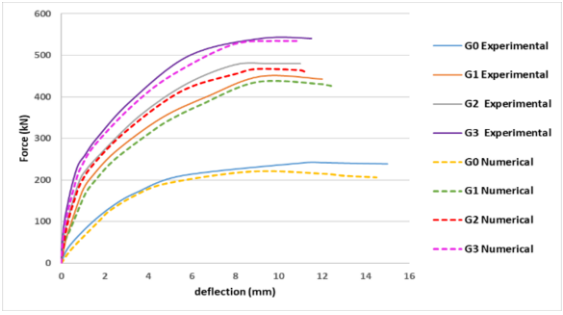

Figure 5. The relationship between load and deflection, both experimentally and numerically, for all four models.

Table 6 presented alternative findings, which detail the percentages of tension concrete damage (d_t%) observed in specimen G3 for each case and load, also it shows the percentages graphically, where regions of high damage intensity are indicated in red and undamaged regions are denoted in blue. The relationship between load and damage intensity indicates that as the burden increases, further strain is exerted on the concrete, steel, and CFRP materials.

Table 6. A Comparison of Slab G3 Damage Patterns

Slab Specimen	Load Multiplier ($\boldsymbol{m_i}$)	Numerical Model	Percentage of Damage ($\boldsymbol{d_t}$%)
G3	1	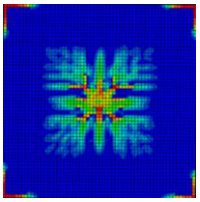	0.17%

Table 6. (Continued) A Comparison of Slab G3 Damage Patterns

Slab Specimen	Load Multiplier (m_i)	Numerical Model	Percentage of Damage (d_t%)
G3	2.25	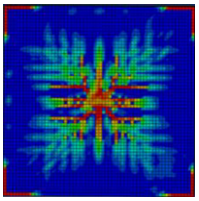	1.2%
	3	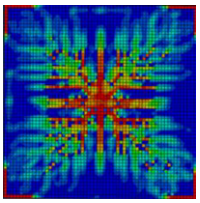	2.6%
	4	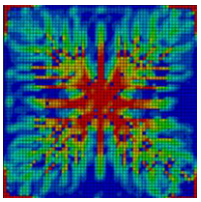	4.9%
	5	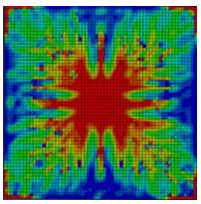	10%

7. Conclusion

The current study concentrates on the CFRP technique utilized to enhance two-way RC slab performance, which is an essential consideration in the process of revitalizing and renovating structures. Based on the analysis of both experimental program and numerical modeling outcomes, the strengthening ratios notably impacted the performance of the reinforced slabs, with an increase in ratio consistently resulting in higher ultimate strength being observed. As well as the augmentation of reinforcement ratios in all three specimens increased initial cracking and a concomitant reduction in deflection. On the other hand, the utilization of CFRP bars for reinforcement resulted in enhanced ultimate strength, reduced cracking width, and enhanced resistance to cracking in comparison to the reference slab, and up until the initial cracking load, all specimens exhibited linear behavior. Additionally, The data shows tension-related concrete damage percentages. As the load increases, damage severity increases. This shows that the added load increases

steel and concrete initial strains. Reflecting plastic damage highlights complementary strain energy, which may be controlled to manage failure and plastic damage. Also, the results demonstrated that CFRP significantly enhances the Pu capacity of slabs. In addition, an extensive level of agreement was observed between the experimental results and the ABAQUS-calibrated numerical models, Thus, confirming the model's efficacy in forecasting the performance of two-way RC slabs that have been strengthened with CFRP rods.

According to numerical results, CFRP bars amounts affect slab behavior. Comparing experimental and computational data shows that CFRP increases the slab's ultimate load capacity, confining the concrete section and supporting shear stress, making it more abrupt and brittle. In general, a reduction in the number of CFRP bars has the potential to increase the extent of red area propagation, which serves as an indicator of possible damage to the steel or concrete. On the contrary, the enlargement of these reddened regions is generally alleviated through the augmentation of the quantity of CFRP bars employed, replicating the consequence noted when reinforcement ratios are decreased. When reduced reinforcement ratios are implemented, such situations lead to increased stresses on structures at lower loads, which ultimately results in structural failure at correspondingly reduced loads.

References

[1] Türer A, Mercimek Ö, Anıl Ö, and Erbaş Y, Experimental and numerical investigation of punching behavior of two-way RC slab with different opening locations and sizes strengthened with CFRP strip, Structures, 2023;49:918–942. doi: 10.1016/j.istruc.2023.01.157

[2] Akhundzada H, Donchev T, Petkova D. Punching Shear Resistance of Flat Slabs Strengthened with Near Surface–Mounted CFRP Bars. J Compos Constr. 2021;25(4):04021035. doi: 10.1061/(ASCE)CC.1943-5614.0001146

[3] Abdel-Kareem AH. Punching Strengthening of Concrete Slab-column Connections Using Near Surface Mounted (NSM) Carbon Fiber Reinforced Polymer (CFRP) Bars. Journal of Engineering Research and Reports 2019;9(2): 1–14. doi:10.9734/JERR/2019/V9I217013.

[4] Hasan Meisami M, Mostofinejad D, Nakamura H. Punching shear strengthening of two-way flat slabs using CFRP rods. 2013; 99:112-122. doi: 10.1016/j.compstruct.2012.11.028.

[5] Behzard P, Sharbatdar MK, Kheyroddin A. Strengthening of Existing RC Two-Way Slabs using New Combined FRP fabric/rod Technique. J Rehabil Civil Eng. 2015;3: 30–44. doi: 10.22075/jrce.2015.368

[6] Foret G, Limam O. Experimental and numerical analysis of RC two-way slabs strengthened with NSM CFRP rods. Constr Build Mater. 2008;22(10): 2025–2030. doi: 10.1016/j.conbuildmat.2007.07.027

[7] Rad MM, Ibrahim SK, Lógó J. Limit design of reinforced concrete haunched beams by the control of the residual plastic deformation. Structures. 2022; 39:987–96. doi: 10.1016/j.istruc.2022.03.080.

[8] Carol I, Rizzi E, Willam K. On the formulation of anisotropic elastic degradation. I. Theory based on a pseudo-logarithmic damage tensor rate. Int J Solids Struct. 2001; 38(4):491–518. doi:10.1016/S0020-7683(00)00030-5.

[9] Rad MM, Papp F, Ibrahim SK, Szép J, Gosztola D, Harrach D. Elasto-plastic analysis and optimal design of composite integral abutment bridge extended with limited residual plastic deformation. Sci Rep. 2023; 13:1-21. doi:10.1038/s41598-023-32787-y.

[10] Gatuingt F, Pijaudier-Cabot G. Coupled damage and plasticity modeling in transient dynamic analysis of concrete. Int J Numer Anal Meth Geomech 2002;26(1):1–24. doi:10.1002/nag.188.

[11] Kratzig WB, Polling R. An elastoplastic damage model for reinforced concrete with a minimum number of material parameters. Comput Struct. 2004;82(15–16):1201–15. doi: 10.1016/j.compstruc.2004.03.002.

[12] Ibrahim SK and Rad MM, Numerical plastic analysis of non-prismatic reinforced concrete beams strengthened by carbon fiber reinforced polymers. in: Proceedings of the 13th fib International PhD Symposium in Civil Engineering, Marne-la-Vallée, Paris, France, 2020, pp. 26–28.

[13] Habashneh M, Movahedi Rad M. Plastic-Limit Probabilistic Structural Topology Optimization of Steel Beams. Appl Math Model 2024; 128:347–369, doi: 10.1016/J.APM.2024.01.029.